American Mineralogist, Volume 84, pages 506–516, 1999

Energetics of kaolin polymorphs

Dominique de Ligny and Alexandra Navrotsky*

Thermochemistry Facility, Chemistry Building, Department of Chemical Engineering and Materials Science, University of California at Davis, Davis, California, 95616, U.S.A.

Abstract

The enthalpy of formation of kaolin polymorphs at 298 K has been determined by drop-solution calorimetry into molten lead borate at 975 K. Corrections have been made for impurities in the samples. The standard enthalpy of formation from the elements is: kaolinite -4120.2 ± 6.6 kJ/mol, dickite -4107.6 ± 5.7 kJ/mol, nacrite -4104.0 ± 7.6 kJ/mol, and halloysite -4097.5 ± 5.6 kJ/mol. Using entropy data from the literature, the standard free energy of formation from the elements at 298 K is -3799.4 ± 6.4 kJ/mol for kaolinite, -3785.1 ± 5.6 kJ/mol for dickite, and -3776.8 ± 5.8 kJ/mol for halloysite. The effect of crystallinity (Hinckley index ranging from 1.6 to 0.4) on the enthalpy of formation of kaolinite is smaller than 5 kJ/mol, the experimental error. The relative stability of the polymorphs probably does not change significantly with pressure and temperature over their range of occurrence. Thus the geological occurrence of halloysite, nacrite, and dickite, which are metastable phases, must be interpreted in terms of kinetics or as the result of a specific synthesis path, rather than as resulting from changes in the thermodynamically stable phase assemblage.

Introduction

Kaolin minerals are dioctahedral clays of 1:1 layer type with chemical composition $Al_2Si_2O_5(OH)_4$. Kaolinite, dickite, and nacrite are polytypes. The kaolinite stacking sequence consists of identical layers with an interlayer shift of $-a/3$. Dickite and nacrite have a two-layer stacking sequence where the vacant site of the octahedral sheet alternates between two distinct sites (Brindley 1980); their interlayer shift is also $-a/3$, but for nacrite the a and b axes are interchanged from those of kaolinite and dickite. The poor crystallinity commonly observed in kaolin minerals is understood as a series of stacking faults. Giese (1988) has shown that no difference occurs within the layers from one polymorph to another and that only the stacking differs. Accordingly, the thermodynamic difference among the polytypes are related mostly to the energy of the interlayer connection.

The strength with which the layers are held together has been related to the orientation of the hydroxyl groups, for which many different structural data are available (Prost et al. 1985; Frost 1997). This orientation is thought to be highly dependent on stacking. The present study of the enthalpy of formation of the polytypes and of several kaolinites with different degrees of stacking disorder provides insight into the magnitude of the interlayer bonding.

In contrast, halloysite is a hydrated polymorph of kaolin with curved layers and a spacing of 10 Å when fully hydrated; the spacing decreases to 7 Å upon dehydration. We studied a 7 Å sample with strong stacking disorder.

Kaolinite, the most abundant polymorph, is found as a weathering product in sedimentary rocks and in hydrothermal systems. Halloysite is found in hydrothermal and surface-weathering deposits. Dickite and nacrite are less common and are restricted to hydrothermal settings. These occurrences have been described by Murray (1988) who presents a review of the genesis of kaolin minerals. The formation of these kaolin minerals may be the result of thermodynamic equilibrium or kinetically limited reaction paths. The enthalpy (and free energy) of formation of each polymorph, as well as the energetics of various kaolinites with different degrees of crystallinity, defines their relative stability. Starting from this thermodynamic base, one can better constrain the conditions of formation of the different polymorphs and, therefore, the history of the sediments and soils that contain them.

Drop-solution calorimetry in molten lead borate at 975 K has become an accepted method for measurement of heat of formation of hydrous phases (Navrotsky et al. 1994) and has been applied to a number of amphiboles (Smelik et al. 1994), micas (Circone and Navrotsky 1992), and zeolites (Kiseleva et al. 1996a, 1996b). Nevertheless, clays present a special challenge both because of their extremely high water content (up to 17 wt%) and because one must deal with natural samples in which water content, chemical purity, and crystallinity all vary. Thus, successful thermochemical study of the kaolin minerals, which are a relatively simple and well-characterized system, is a prelude to the study of more complex clays. Previous calorimetric studies exist for kaolinite, dickite, and halloysite (Barany and Kelley 1961; Hemingway et al. 1978) and provide a basis for comparison.

* E-mail: anavrotsky@ucdavis.edu

0003–004X/99/0004–0506$05.00

METHODS

Kaolinite samples

Four samples of kaolinite were studied. Two Georgia kaolinites, the well-ordered KGa-1 and the poorly ordered KGa-2, were obtained from the Source Clay Repository of the Clay Minerals Society (described by Van Olphen and Fripiat 1979). A third Georgia kaolinite sample was obtained from J. Chermak. It is a well-ordered sample from Wilkinson County, Georgia (described in Brindley et al. 1986). This bulk sample was separated into different size fractions. The bulk sample (Wlk-bk) and the 2–10 (Wlk-10) and 0.1–1 (Wlk-1) μm (sphere diameter equivalent) fractions were studied. The 2–10 and 0.1–1 μm size fractions constitute 44 and 30 wt% of the bulk sample, respectively. The last sample, API no. 9, is a kaolinite from Alta Mesa, New Mexico. Barany and Kelley (1961) used this sample to determine the enthalpy of formation of kaolinite.

Dickite, nacrite, and halloysite samples

The dickite sample was obtained from Ward's National Science Establishment, Inc. and is from a deposit near San Juanito, Mexico [the same locality as the material studied by Barany and Kelley (1961)]. A low-temperature infrared study by Prost (1984) identified some nacrite mixed with the San Juanito dickite but the amount was not quantified. The nacrite sample was obtained from M.D. Buatier who hand picked the crystals, removed dolomite and calcite with 5N HCl, and washed the product with distilled water by centrifugation. This nacrite occurs in the Lodève Permian basin (France), as described in Buatier et al. (1996). The halloysite used in this work was separated by sedimentation and centrifugation by G.Y. Jeong and was formed by weathering of anorthosite in Sancheong, Korea (Jeong and Kim 1993, 1996).

Other samples

To complete the thermochemical cycles, some oxides were also studied. Fe_2O_3 from Johnson Matthey, Puratronic 99.999%; SiO_2 quartz from Baker certified at 99%; Al_2O_3 99.97% from Alpha AESAR; and gibbsite from Baker certified at 99%. The water content of gibbsite was checked by thermogravimetric analysis (TGA). A weight loss of 34.53% was found for the combined dehydroxylation at 580 and 820 K in agreement with the literature and the theoretical weight loss of 34.64% (Brindley and Nakahira 1959).

Composition and characterization of the clay samples

The chemical composition of all samples has been determined using a Cameca SX-50 fully automated electron microprobe (EMP) at the Princeton Materials Institute, Princeton University. The samples were dehydroxylated at 1770 K, compacted, and mounted with epoxy in a sample holder and polished. The water content was obtained separately using a Netzsch TGA 409 thermogravimetric analyzer. The thermogram was obtained by heating 50 mg of sample to 1370 K in static air at a rate of 10 K/min. A buoyancy correction necessary with this instrument diminishes the accuracy. The total weight loss determined by weighing the TGA crucible before and after the TGA experiment, which is considered a more accurate method, confirmed the result of the TGA within 0.2 wt%. Thus the uncertainty in water content is ±0.2 wt%. The chemical compositions presented in Table 1 were determined by renormalizing the microprobe analyses using the measured total weight loss as water content. The sample of dickite was also analyzed by coupling the thermogravimetric study with mass spectrometry (MS-Cube from Balzers). Gas evolved from the sample on the TGA balance was fed directly into the mass spectrometer, which detected SO_2 between 1170 and 1270 K. The small associated weight loss was too spread-out in temperature to be quantified properly. Nevertheless, this observation confirms the presence of sulfur in the dickite (attributed to alunite, see below).

X-ray diffraction (XRD) patterns were accumulated during continuous scans of 1°/min between 5 and 70° (2θ) on a Scintag PAD 5 diffractometer with Cu$K\alpha$ radiation. The region between 15 and 30° is presented in Figure 1. This region has been used to measure the Hinckley index following Brindley (1980, Table 3).

The positions of the main reflections of quartz and anatase are noted in Figure 1. Some anatase can be detected in Wlk-bk, KGa-1, and KGa-2 and some quartz in API no. 9. No other crystalline impurities have been identified. Wlk-1 showed sharp kaolinite peaks above a continuous ''hump'' from 15 to 40°, suggesting the presence of some amorphous impurity.

From the chemical analysis, the amount of impurities can be deduced using the theoretical Si/Al and Si/H_2O ratios of $Al_2Si_2O_5(OH)_4$. Therefore it is assumed that the sample is stoichiometric. Any excess compared to this ratio was attributed to impurity phases. In the thermochemical calculations, the impurities were taken as the corresponding oxides. The estimated impurities on a weight percent basis are presented in Table 2.

Adsorbed water

The most important impurity with regard to enthalpy measurements is adsorbed water, which is sensitive to relative humidity. The samples were kept in the controlled atmosphere of the laboratory at 296 K and 50% relative humidity. We determined the amount of adsorbed water in two ways: the stoichiometric procedure followed in constructing Table 2 and by using the low temperature region of the thermogravimetric curves. Figure 2 presents a close-up of this region for all samples except halloysite. The amount of adsorbed water was taken at the inflection point of the thermogram, around 523 K for most of the samples.

The value for halloysite comes from the TGA of Figure 3, in which the sample has been heated to 523 K and left at this temperature for several hours to reach equilibrium

TABLE 1. Composition of kaolin minerals in weight percent determined by electron microprobe analysis of dehydroxylated samples

	Wlk-bk	Wlk-1	Wlk-10	API#9	KGa-1	KGa-2
SiO_2	45.95 (0.31)	42.98 (0.40)	45.7 (2.25)	47.18 (1.95)	45.28 (0.84)	44.44 (0.74)
Al_2O_3	39.49 (0.51)	36.65 (0.60)	38.24 (1.65)	38.17 (2.00)	39.1 (1.04)	38.1 (0.47)
TiO_2	0.07 (0.14)	5.59 (0.54)	1.69 (3.75)	0.45 (0.60)	1.1 (1.38)	1.88 (0.84)
H_2O+*	14.16 (0.2)	13.81 (0.2)	13.98 (0.2)	13.82 (0.2)	13.95 (0.2)	14.24 (0.2)
Fe_2O_3 (T)	0.13 (0.09)	0.46 (0.31)	0.16 (0.13)	0.17 (0.18)	0.16 (0.12)	0.95 (0.32)
MgO	0.02 (0.04)	0.04 (0.06)	0.02 (0.02)	0.03 (0.04)	0.03 (0.03)	0.03 (0.03)
CaO	0.03 (0.03)	0.09 (0.03)	0.03 (0.02)	0.03 (0.05)	0.05 (0.04)	0.03 (0.04)
Na_2O	0.14 (0.13)	0.35 (0.05)	0.14 (0.08)	0.08 (0.03)	0.32 (0.19)	0.27 (0.08)
K_2O	0.03 (0.03)	0.03 (0.03)	0.03 (0.03)	0.05 (0.04)	0.02 (0.02)	0.05 (0.04)

Notes: The numbers in parentheses are errors associated with the analyses and represent the standard deviation of at least 15 microprobe analyses.
* The total water content was determined as the weight loss during firing.

before being heated further. This mimics the calorimetric procedure adopted for this sample.

A comparison of the amount of adsorbed water deduced from these two methods is shown in Table 3. Generally the TGA value is slightly lower than the stoichiometric value, probably due to the inaccuracy introduced by the inflection point estimate. The difference is less than 0.2 wt%, except for dickite. These small differences show the data are reliable, particularly given that the stoichiometric approach is very sensitive to the measured Al/Si ratio.

For dickite, the 1 wt% excess water predicted by the measured Al/Si is not detected in the TGA record of Figure 2. The presence of excess Al_2O_3 could be interpreted as gibbsite, but because no dehydroxylation is seen around 570 K, gibbsite cannot be responsible for the excess water. The coupled TGA mass spectroscopy experiment allowed detection of some degassing of SO_2 above 1200 K with a weight loss around 0.5 wt%. Barany and Kelley (1961) reported some sulfur trioxide for a sample coming from the same locality. Therefore, the total excess of Al_2O_3, K_2O, and Na_2O and the weight loss can be assigned to alunite, $(Na,K)Al_3(OH)_6(SO_4)_2$, a mineral commonly associated with dickite. Alunite typically loses its water at 825 K and sulfur oxide at 1125 K. The first reaction is concomitant with dickite dehydroxylation and the second reaction is sluggish. The thermogram is not in contradiction with the presence of alunite.

The adsorbed water content is related to the surface area of the clay. The surface area of some of the samples has been measured by N_2 adsorption by the Brunauer-Emmett-Teller (BET) method (Table 3). The degree of coverage, θ, is defined as the number of water layers covering the clay assuming that one molecule of water covers 10.8 $Å^2$ (Iwata et al. 1989) and is nearly constant for the kaolinite samples. The inconsistent data obtained for dickite compared to the kaolinites supports the contention that the 1 wt% of weight loss in dickite is associated with SO_2 and not chemisorbed water.

Calorimetric measurements

The enthalpies of formation were determined using a Tian Calvet high-temperature heat-flux microcalorimeter described in detail by Navrotsky (1997). Drop-solution calorimetric methods (Chai and Navrotsky 1993; Navrotsky et al. 1994) were chosen to avoid decomposition of the clays at the calorimeter temperature prior to dissolution. Calorimetric experiments were performed using pressed pellets between 14 and 16 mg in mass. The samples were dropped from room temperature into molten $2PbO \cdot B_2O_3$ at 975 K. As described previously for hydrous samples (Navrotsky et al. 1994), an Ar flow of 100 mL/min was maintained in the calorimeter. The calorimetric signal returned to baseline within 90 min.

The very high level of adsorbed water in halloysite caused the pellet to explode due to the sudden release of vapor. To overcome this difficulty, the pellet was first heated at 523 K above the calorimeter in a small hanger equipped with a thermocouple (McHale et al. 1997). The weight of the water lost was subtracted from the room temperature weight using data from the TGA experiment (Fig. 3). The sample was dropped one hour after introduction at 523 K so that its water content was that of the equilibrated plateau of Figure 3.

The calorimeter was calibrated by the measurement of the heat content of small platinum pieces, which produced a comparable heat effect to the 15 mg kaolin samples.

RESULTS

Measured enthalpies of drop solution

The drop-solution calorimetric results for the kaolin minerals, ΔH_{ds}, are summarized in Table 4. Pure quartz, corundum, hematite, and gibbsite were studied under the same conditions (Table 5). Before we can correct the raw data for impurities, the enthalpy of drop solution for the individual impurities must be determined. The enthalpy of drop solution for anatase and alunite were determined with the thermodynamic cycles shown in the Appendix table. The values of drop-solution enthalpies for the other impurities are taken from previous work in our laboratory. All the values used are given in Table 5.

In this study two kinds of water can be distinguished, liquid water and adsorbed water. The enthalpy of drop solution of liquid water can be found by a cycle involving gibbsite (see Appendix table). The value obtained through

TABLE 1—*Extended*

Dickite	Nacrite	Halloysite
45.8 (0.52)	46.3 (1.15)	43.02 (0.44)
39.27 (0.49)	38.79 (1.14)	37.79 (0.53)
0.02 (0.05)	0.02 (0.05)	0.03 (0.13)
14.74 (0.2)	14.53 (0.2)	17.63 (0.2)
0.02 (0.06)	0.05 (0.10)	0.18 (0.12)
0.02 (0.02)	0.03 (0.04)	0.11 (0.06)
0.04 (0.11)	0.12 (0.17)	0.16 (0.11)
0.09 (0.07)	0.15 (0.16)	0.71 (0.27)
0.02 (0.02)	0.03 (0.03)	0.37 (0.08)

the cycle is found to be 69.6 ± 1.1 kJ/mol, which is close to the value of 70.2 ± 2.7 first determined by Navrotsky et al. (1994). The enthalpy of drop solution of water, assuming all the H_2O is evolved and does not interact with the melt, is just its heat content, H_{975}-H_{298}. This value, 69.0 kJ/mol (Robie and Hemingway 1995), is in good agreement with our experimental measurement, and has been used in further calculations.

The enthalpy of drop solution of adsorbed water can be obtained by adding the enthalpy of adsorption of water to the heat content of free liquid water. The adsorption calorimetry results of Iwata et al. (1989) were used. The degree of coverage of our samples (Table 3), corresponds well with a degree of coverage of 1.25 derived from the adsorption isotherm of Iwata et al. (1989) at our experimental humidity conditions, 50% relative humidity at 296 K. Therefore, samples in the two studies can be presumed to be similar. The enthalpy of adsorption was obtained by integrating the curve of the differential heat of adsorption given in Iwata et al. (1989) between a degree of coverage of 0 and 1.25. The value obtained (Table 5) is in good agreement with the value that can be deduced from the enthalpies of immersion given by Fripiat et al. (1982).

Correction of the data for impurities

The ΔH_{ds}^{no} value of Table 4 corresponds to the ΔH_{ds} value normalized to 1 mole of pure kaolinite, given the amount of impurities shown in Table 3. Accordingly, the formula of the sample can be written: $Al_2Si_2O_5(OH)_4$,(Σ x_i impurity), where the molar amount of impurity, x_i, is derived from the microprobe analysis.

The experimental data have been corrected following the cycle:

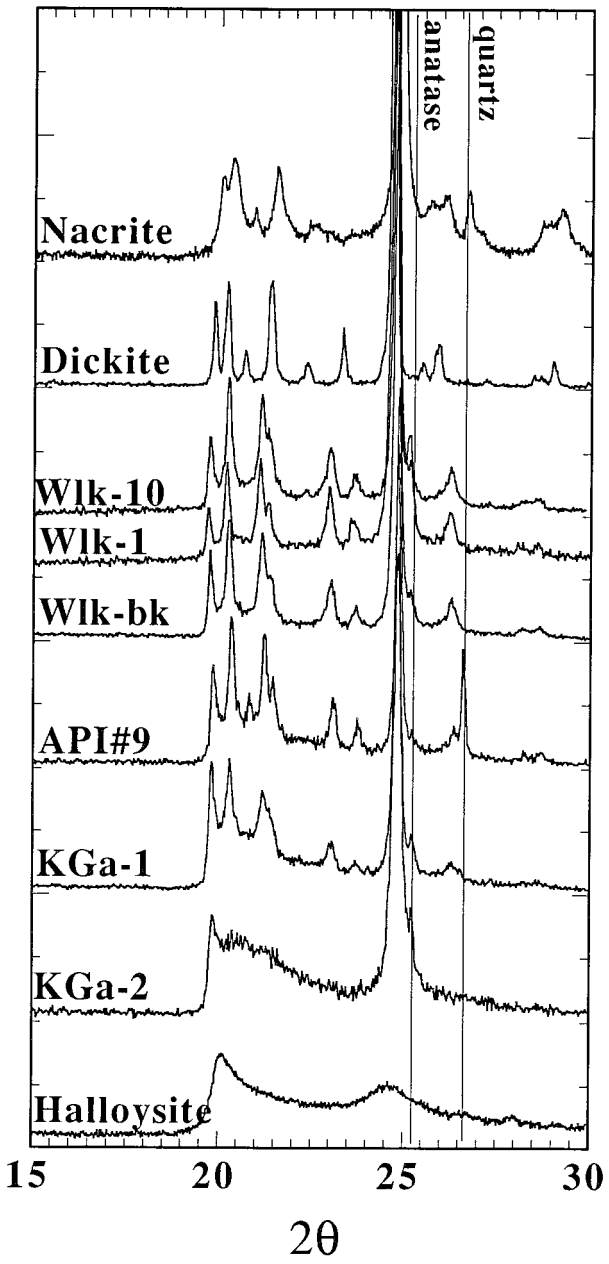

FIGURE 1. X-ray diffraction patterns of kaolin minerals. The location of the main reflection of quartz and anatase are shown for impurity identification. The shift of baseline for Wlk-1 is associated with the presence of an amorphous phase. (Cu$K\alpha$ radiation).

$$\begin{aligned} Al_2Si_2O_5(OH)_4, \left(\sum x_i \text{ impurity}\right) (298\text{ K}) &= \text{Oxides (sol, 975 K)} && \Delta H_{ds}^{no} \\ \text{Oxides (298 K)} &= \text{Impurity (sol, 975 K)} && -\Delta H_{ds}^{i} \\ Al_2Si_2O_5(OH)_4 (298\text{ K}) &= \text{Oxides (sol, 975 K)} && \Delta H_{ds}^{co} \end{aligned}$$

$$\Delta H_{ds}^{co} = \Delta H_{ds}^{rm} - \sum_{i=\text{imp.}} x_i \Delta H_{ds}^{i}.$$

TABLE 2. Impurities present in the kaolin minerals on a weight percent basis

	Wlk-bk	Wlk-1	Wlk-10	API#9	KGa-1	KGa-2	Dickite	Nacrite	Halloysite
SiO_2	0.00	0.00	0.70	2.19	0.00	0.00	0.00	0.57	0.00
Al_2O_3	0.51	0.19	0.00	0.00	0.69	0.40	0.42	0.00	1.30
TiO_2	0.07	5.59	1.69	0.45	0.10	1.88	0.03	0.02	0.13
Fe_2O_3 (T)	0.13	0.46	0.16	0.17	0.16	0.95	0.02	0.05	0.23
MgO	0.02	0.04	0.02	0.03	0.03	0.03	0.02	0.03	0.11
CaO	0.03	0.09	0.03	0.03	0.05	0.03	0.04	0.12	0.16
Na_2O	0.14	0.35	0.14	0.08	0.32	0.27	0.09	0.15	1.01
K_2O	0.03	0.03	0.03	0.05	0.02	0.05	0.02	0.03	0.21
H_2O	0.38	0.92	0.46	0.33	0.37	0.91	1.00	0.82	4.73

Table 4 shows the contributions due to impurities and the corrected enthalpies of drop solution.

For the halloysite, because of the preheating stage, the impurity correction and the final drop-solution enthalpy were calculated as follows:

Halloysite, impurity (xl, 523 K)

= Oxides (sol, 975 K) This study

oxides (sol, 975 K)

= impurity (xl, 298 K) This study

impurity (xl, 298 K)

= impurity (xl, 523 K) Robie and Hemingway 1995

Halloysite (xl, 298 K)

= Halloysite (xl, 523 K) Robie and Hemingway 1995

Halloysite (xl, 298 K)

= oxides (sol, 975 K) $\overline{\Delta H^{\text{co}}_{\text{ds}}}$.

The heat capacity of halloysite has not been measured previously at 298 to 523 K. The heat capacity of the different polymorphs has been studied at low temperatures by King and Weller (1961). In the interval from 50 to 300 K, the heat capacity of kaolinite and halloysite differ by less than 0.7%. The very small differences at low temperature suggest that the differences will be even smaller at higher temperature. Accordingly, we used the value of heat capacity for kaolinite reported in Robie and Hemingway (1995) to estimate the heat content of halloysite between 298 and 523 K.

The uncertainty of the impurity correction was determined as follows. Assuming that uncertainty of the microprobe analysis, ΔX_i, is gaussian, the error can be calculated as:

$$\Delta(\Delta H^{\text{co}}_{\text{ds}}) = \sqrt{[\Delta(\Delta H^{\text{no}}_{\text{ds}})]^2 + \sum_{i=\text{imp.}} x_i^2[\Delta(\Delta H^{i}_{\text{ds}})]^2 + \sum_{i=\text{imp.}} (\Delta H^{i}_{\text{ds}})^2 \Delta x_i^2}.$$

Except for quartz and anatase, for which we have direct X-ray determination, we assumed that the other impurities were present as oxides. We realize this is improbable for the alkalis and for Al_2O_3. Brindley et al. (1986) showed that Fe in kaolin is mostly structural and substitutes for Al in the octahedral site. This has been confirmed by Schroeder and Pruet (1996) who showed a clustered distribution of Fe in kaolinite. However, the magnitude of the correction introduced by each of these impurity oxides individually is smaller than the error of the measurements, and there is no unique way of linking the correction terms to assumed substitution mechanisms.

In the case of dickite, the impurities (H_2O, SO_2, Na_2O, Al_2O_3, and K_2O) are associated with the presence of al-

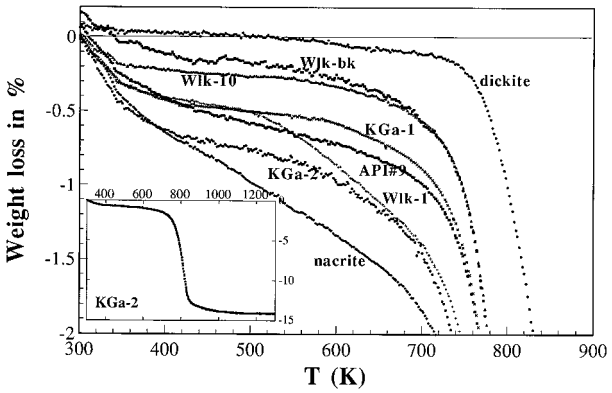

FIGURE 2. Low temperature part of the thermogravimetric analysis curves of the kaolin minerals. The samples were previously compressed into pellets (10 K/min heating rate, static air).

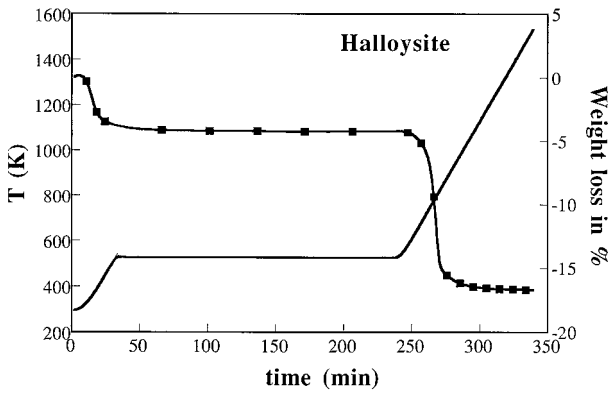

FIGURE 3. Thermogravimetric analysis curve of halloysite simulating the pre—heating stage inside the calorimeter. The two heating ramps at 10 K/min are separated by a constant temperature plateau of 4 h.

Table 3. Adsorbed water and physical properties of the samples

	Wlk-bk	Wlk-1	Wlk-10	API#9	KGa-1	KGa-2	Dickite	Nacrite	Halloysite
H_2O-Stoc.*	0.38	0.92	0.46	0.33	0.37	0.91	1.00	0.82	4.73
H_2O-TGA†	0.31	0.42	0.26	0.53	0.45	0.64	0.09	0.52	4.50
Hinck.	1.5	1.9	1.6	1.4	1.0	0.4			
BET m^2/g	7.6	nd	nd	11.5	11.4	19.2	1.0	nd	nd
θ	1.4 ± 0.3	nd	nd	1.1 ± 0.2	1.1 ± 0.2	1.8 ± 0.4	36.0 ± 7‡	nd	nd

Notes: Hinck. = the Hinckley index determined from the X-ray data of Figure 1. BET = specific surface determined by BET. θ = degree of coverage. nd = no data.

* Adsorbed water determined by stoichiometric consideration from the compositions of Table 1 (in weight %).

† Adsorbed water determined by TGA in weight %.

‡ Value obtained by attributing the weight loss to H_2O instead of SO_2 (see text).

Table 4. Enthalpies of drop solution of kaolin minerals at 975 K in $2PbO{\cdot}B_2O_3$ and derived standard enthalpies of formation

	Wlk-bk	Wlk-1	Wlk-10	API#9	KGa-1	KGa-2	Dickite	Nacrite	Halloysite
ΔH_{ds}	1.439	1.360	1.439	1.420	1.436	1.441	1.421	1.395	1.307
±*	0.010	0.019	0.020	0.007	0.008	0.007	0.013	0.018	0.011
ΔH_{ds}^{no}	376.4	380.2	384.0	379.2	381.0	389.5	373.0	366.6	348.5
SiO_2 quartz	0.0	0.0	1.2	3.7	0.0	0.0	0.0	0.9	0.0
Al_2O_3 α	1.4	0.6	0.0	0.0	1.9	1.1	0.0	0.0	3.8
TiO_2 anatase	0.1	9.8	2.8	0.8	1.8	3.2	0.0	0.0	0.2
Ca,Mg,Na,K	−0.7	−2.0	−0.8	−0.7	−1.5	−1.5	0.0	−0.8	−5.9
Fe_2O_3 α	0.3	1.3	0.4	0.5	0.4	2.6	0.0	0.1	0.6
H_2O ads.	4.7	12.1	5.8	4.2	4.6	11.6	0.0	10.2	0.0
Alunite	0.0	0.0	0.0	0.0	0.0	0.0	13.3	0.0	0.0
Total (impurities)	5.8	21.8	9.4	8.5	7.2	17.0	13.3	10.4	−1.3
ΔH_{ds}^{co}±	370.6	358.3	374.7	370.7	373.7	372.5	359.7	356.3	349.8
	3.9	5.9	10.2	7.1	5.2	3.9	4.5	6.4	4.3
ΔH_f^{oxides}	−49.6	−37.4	−53.7	−49.7	−52.8	−51.5	−38.9	−35.3	−28.8
±	4.7	6.5	10.5	7.6	5.9	4.8	5.3	6.9	5.1
$\Delta H_f^{elements}$	−4118.3	−4106.1	−4122.4	−4118.4	−4121.5	−4120.2	−4107.6	−4104.0	−4097.5
±	5.3	6.9	10.8	8.0	6.4	5.4	5.7	7.6	5.6

Notes: The experimental data ΔH_{ds} is presented in the first line in kJ/g. This value has been normalized at one mol of $Al_2Si_2O_5(OH)_4$,(Σimp.) to give ΔH_{ds}^{no} expressed in kJ/mol. The contribution to ΔH_{ds} from each impurity is also given based on data in Table 5. The corrected result for the pure phase is ΔH_{ds}^{co}. The molecular weight used is 258.160 g/mol.

* The error basrs of ΔH_{ds} are given as: $\Delta(\Delta H_{ds}^{m}) = 2\sigma/\sqrt{n-1}$ where σ is the standard deviation and n the total number of experiments ($n \geq 6$).

Table 5. Enthalpies of drop solution of oxides or impurities at 975 K in $2PbO{\cdot}B_2O_3$

	ΔH_{ds} (kJ/mol)	±*	Reference
Al_2O_3 corundum	107.2	1.0	This study
$Al(OH)_3$ gibbsite	184.5	0.7	This study
CaO lime	−17.4	0.9	Kiseleva et al. 1996
Fe_2O_3 hematite	160.1	1.1	This study
H_2O liquid	69.0	1.1	Robie ahd Hemingway 1995
H_2O adsorbed	85.0	2.0	Calculated from Iwata 1989
K_2O	−193.7	1.1	Kiseleva et al. 1996
$KAl_3(OH)_6(SO_4)_2$	1391	5	Calculated from Robie and Hemingway 1995
MgO periclase	36.5	1.0	Smelik et al. 1994
Na_2O	−113.1	0.8	Kiseleva et al. 1996
O_2 gas	21.8	0.2	Robie and Hemingway 1995
SO_2 gas	33.0	0.3	Robie and Hemingway 1995
SiO_2 quartz	37.9	0.6	This study
TiO_2 rutile	55.4	1.2	R.L. Putnam (pers. com.)
TiO_2 anatase	50.1	1.2	Calculated from R.L. Putnam (pers. com.)

* 2 standard deviations of the mean.

unite, as discussed previously. However, thermodynamic data are available only for the potassic end-member. The difference in molecular weight between the sodic and potassic end-members of alunite is small. Moreover, the enthalpy of formation from the elements of sodium hydroxide or sodium sulfate is of the same magnitude as their potassic counterpart. The values of drop-solution enthalpies of the potassic and sodic end-members would therefore probably be similar. Accordingly, all of the alunite has been considered as the pure potassic end-member. The uncertainties introduced by this approximation are not a significant source of error.

For halloysite, the individual corrections are larger. The impurities could have been present as another silicate phase such as a feldspar or illite. However, this would significantly change the actual Al/Si ratio of halloysite and require the existence of the feldspar above the probable level of detection of the XRD pattern (about 5%). Because the correction for the alkali elements is compensated by that for corundum and hematite (Table 4), we

conclude that our method of correction for the impurities as oxides is appropriate and corrections generally lie within the experimental error.

In Wlk-1, an amorphous phase was suggested by the XRD data. The amount and composition of this phase are difficult to estimate but the amount probably lies between about 5 and 15%. Therefore the composition of the clay may also differ from the bulk composition. Our inability to make the proper correction for the amorphous phase is thought to be responsible for the smaller value of heat of formation obtained in Wlk-1 compared to the other kaolinites. Accordingly, this sample has been excluded from the calculation of heat of formation of pure kaolinite.

Enthalpy of formation

We first determined the enthalpy of formation of each clay from the oxides using the enthalpy of drop solution of each oxide (Table 5). We then calculated the enthalpy of formation from the elements using data from Robie and Hemingway (1995) (see Table 4). The uncertainties increase at each step because of the combined uncertainties introduced by the enthalpy of drop solution of the oxides and their enthalpy of formation from the elements.

The values in Table 5 are consistent with the results obtained previously in our laboratory, with the exception of the enthalpy of drop solution of quartz, which is 1 to 2 kJ/mol lower. This small discrepancy may be related to the sample or some other experimental differences.

Within experimental uncertainty, the enthalpies of drop solution do not appreciably change from one kaolinite to another, as shown in Figure 4 (after omitting Wlk-1 as discussed previously). The enthalpy of formation from oxides of kaolinite is taken as the mean of all the samples: -51.5 ± 5.9 kJ/mol. Among the different polymorphs, the enthalpic stability decreases in the sequence: kaolinite, dickite, nacrite, and halloysite.

The Gibbs free energy of formation can now be determined for kaolinite, dickite, and halloysite taking the entropy at 298 K from King and Weller (1960): 202.9 ± 1.3, 197.1 ± 1.3, and 203.3 ± 1.3 J/mol·K, respectively. Robie and Hemingway (1991) report also an entropy at 298 K of 200.9 ± 0.5 J/mol·K for KGa-1. The difference of entropy from the two studies has a very small effect on the Gibbs energy of formation for kaolinite: -3799.4 ± 6.4 kJ/mol and -3798.8 ± 5.2 kJ/mol using King and Weller (1960) and Robie and Hemingway (1991), respectively. This free energy value is identical to that compiled in Robie and Hemingway (1995) from the experimental data of Barany and Kelley (1961). However the free energies of dickite (-3785.1 ± 5.6 kJ/mol) and halloysite (-3776.8 ± 5.8 kJ/mol) are greater than those found in Robie and Hemingway (1995), -3796.0 ± 2.1 kJ/mol and -3780.7 ± 10.0 kJ/mol, respectively. The higher value for dickite may come from the alunite correction, since Barany and Kelley (1961) did not consider the presence of alunite in a sample of similar origin. Using the experimental drop-solution data for dickite without the alunite correction yields -3792.3 kJ/mol, which is closer to the value listed in Robie and Hemingway (1995).

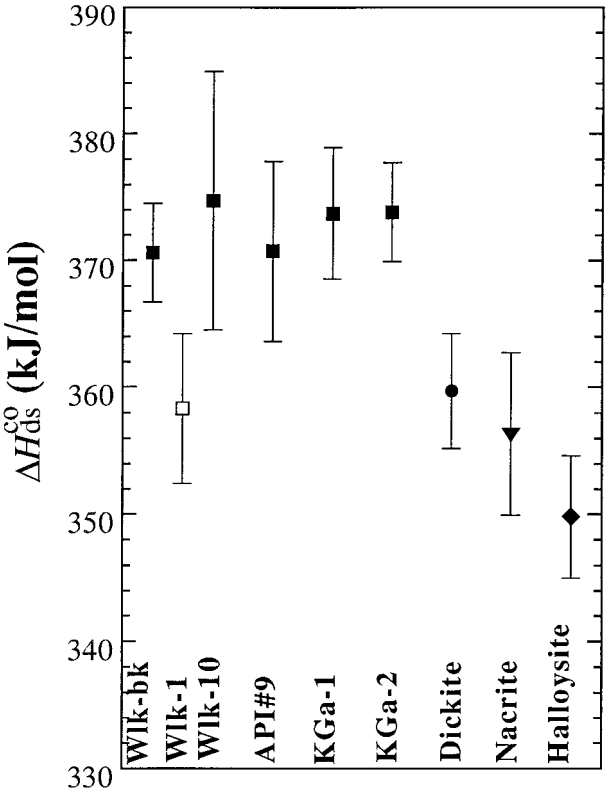

FIGURE 4. Enthalpies of drop solution of the different kaolin minerals, and their associated error bars. The kaolinites are arranged according to their crystallinity along the *x* axis.

The absence of entropy data for nacrite prevents us from determining its Gibbs free energy of formation. However, the difference in entropy between dickite and kaolinite shows that the Gibbs free energy is mostly affected by the enthalpy of formation. Therefore the Gibbs free energy for nacrite should be roughly equal to that of dickite.

DISCUSSION

The enthalpy of formation found for kaolinite and the data reported in the literature (Table 4) are in good agreement, as are the uncorrected value for dickite and the value derived by Robie and Hemingway (1995) from Barany and Kelley (1961). These results support the validity of drop-solution calorimetry in molten lead borate at high temperature for the determination of the enthalpy of formation of clay minerals. Although our enthalpy and Gibbs free energy for kaolinite and halloysite are within the error of the previous data, the Gibbs energy for dickite is significantly more endothermic. We conclude from our study that dickite is metastable with respect to kaolinite.

A recent investigation of the Gibbs energies of formation by Zotov et al. (1998) by acid dissolution in hydrothermal conditions is in disagreement with the results

presented here (Table 6). If the value measured for kaolinite is the same in both studies, the value for dickite presented by Zotov et al. (1998) implies that dickite is stable with respect to kaolinite. The experimental method used by Zotov et al. (1998) has several known limitations: (1) the activity coefficients of solute ions in hydrothermal conditions are not well known; (2) the equilibrium is difficult to define when reversal experiments are not performed and; (3) incongruent dissolution can introduce several new phases. In contrast, the only limitation of our study is related to the sample purity. It could be argued that the correction applied to the dickite sample in this study is not appropriate. However, if the correction is ignored, the Gibbs free energy would be −3792.1 kJ/mol whereas if the correction is done only on an oxide basis, i.e., without the presence of alunite as for the other samples, the free energy of dickite would be −3788.1 kJ/mol. In all these cases, kaolinite (−3799.4 ± 6.4 kJ/mol) is calculated to be more stable than dickite in this study. As previously mentioned, the San Juanito sample could contain some nacrite (Prost 1984). Using the enthalpy data of Zotov et al. (1998) for dickite and the data from this study for nacrite, we estimate that the samples studied contain 81% nacrite. This is highly unlikely. Indeed, the San Juanito dickite is commonly used as a reference dickite (Frost 1997). A difference between this study and that of Zotov et al. (1998) is that the sample in this study was dry and the sample studied by Zotov et al. (1998) was in a fully hydrated state. The Gibbs energy of formation from the elements determined by Zotov et al. (1998) should be corrected by the Gibbs free energy of hydration of the kaolinite and dickite. A significant difference in the Gibbs free energy may indicate that the polytypes have very distinct free energies of hydration. This clearly needs further study.

At room temperature the order of decreasing stability of kaolin polymorphs is: kaolinite, dickite, nacrite, and halloysite 7Å. This order should remain the same at higher temperature or at higher pressures, within the range where clays exist stably. The small difference in heat capacity and entropy (King and Weller 1961) and the nearly identical volumes of the different polytypes support this view. The volumes for kaolinite, dickite, and nacrite are 99.33, 99.71, and 99.05 cm^3/mol, respectively (Bish and von Dreele 1989; Zheng and Bailey 1994). The thermochemical data suggest there is no thermodynamic stability field for any polymorph other than kaolinite. Thus one needs to explain the genesis of other polymorphs in terms of kinetics as already proposed by Anovitz et al. (1991). Based on field observation, Ehrenberg et al. (1993) proposed a phase diagram with a stability field for dickite at high temperature. This stability field seems unlikely since the difference of entropy (King and Weller 1991) will favor kaolinite with respect to dickite at high temperature. The dissolution of kaolinite and formation of dickite at 380 K (Ehrenberg et al. 1993) cannot be explained by our measurements, but dissolution-reprecipitation in an open system may be controlled kinetically.

For the halloysite 7 Å, Singh (1996) and Singh and Mackinnon (1996) present a mechanism of halloysite formation by kaolinite exfoliation. Their proposed mechanism is a typical kinetically limited formation of a metastable phase. The halloysite 10 Å could be stabilized by the presence of interlayer water. However, the enthalpy of water adsorption on halloysite needs to be measured to test this possibility.

The enthalpy difference among the samples (halloysite excepted) is related to the interlayer differences. The polytypism is a long-range organization of the same interlayer spaces. The crystallinity increases with the extension of coherent stacking domains. Understanding the link between local structure and energy should help to constrain the occurrence conditions.

The Hinckley index has been proposed as an empirical estimate of the degree of crystallinity. A more rigorous theoretical basis for the reliability of this index can be found in the numerical model proposed by Artioli et al. (1995) who correlate the Hinckley index to a density of stacking faults. The biggest enthalpy difference observed between the kaolinite samples is 4 kJ/mol (excluding Wlk-1). The insensitivity of the kaolinite enthalpy of formation to crystallinity (Hinckley range 0.4–1.9) contradicts the energy calculation of Artioli et al. (1995). The electrostatic energy calculation gave a difference of 12.4 kJ/mol between an ordered B-layer kaolinite and one comprised of the superposition of different layer types, (B, C, and their enantiomorphic forms). Our results suggest that the density of stacking faults in a kaolinite does not strongly affect its enthalpy of formation. A similar observation has been made by Clemens et al. (1987), who reported that stacking disorder in phlogopite had a very small effect on thermodynamic properties (within their experimental error of 4 kJ/mol).

The effect of the degree of crystallinity (i.e., order) on the stability of clay minerals is illustrated by the Kittrick (1966) study on kaolinite. Kittrick (1966) suggested that the Gibbs free energy of formation of kaolinite varied by at least 6.3 kJ/mol with the degree of crystallinity. Because the configurational entropy arising from stacking defects is negligible, our result predicts that the Gibbs free energy varies by less than about 4 kJ/mol with the degree of crystallinity. To characterize his trend Kittrick (1966) excluded four samples. Moreover, even within the six samples he used to determine his trend, two with the same crystallinity (in the sense of Hinckley) differ by 4 kJ/mol. Accordingly the variations seen by Kittrick (1966) appear to lie within experimental error. Nevertheless, his and our results are in agreement with a maximum energetic effect of 4–6 kJ/mol associated with the degree of crystallinity in kaolinite.

An unexpected aspect of our study is the relatively large enthalpy difference between polytypes compared to the small effect from order. This difference is even more striking when one considers that large crystals of dickite commonly occur in nature, even when poorly ordered kaolinite is apparently more stable.

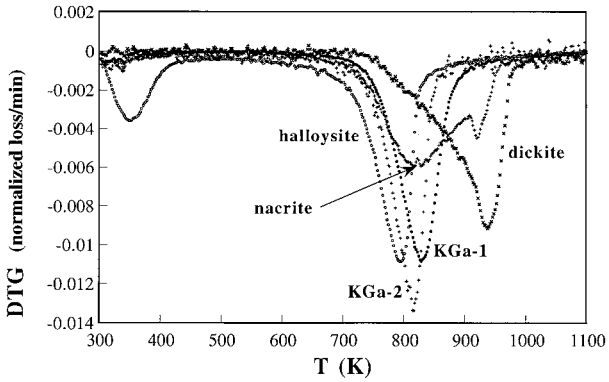

FIGURE 5. Differential thermogravimetric analysis curves of the kaolin minerals. The first peak around 370 K corresponds to adsorbed water on halloysite (10 K/min heating rate, static air).

The individual layers of kaolinite, dickite, and nacrite are very similar to one another, and the matching of adjacent corrugated surfaces are equivalent (Giese 1988; Bookin et al. 1989). Vibrational studies, however, reveal discriminating features among the polymorphs. The hydroxyl stretching region has been interpreted in different ways. Prost et al. (1985) reported that inner-surface hydroxyls are involved in stronger hydrogen bonds in dickite than in kaolinite, whereas Brindley et al. (1986) and Frost (1997) suggested the opposite. Testing interlayer cohesion by intercalation of hydrazine, Cruz-Cumplido et al. (1982) noticed that the expandability of kaolinite increased with the number of defects, and that dickite did not expand at all. They therefore concluded that well-ordered kaolinites have a greater degree of interlayer cohesion than the low-ordered kaolinites and that dickite has very strong interlayer cohesion.

The insensitivity of enthalpy to order (i.e., the degree of crystallinity) suggests that interlayer cohesion is not readily correlated with the relative energetic stability. We did not determine the energetics of the hydrogen bond in the different polytypes, but rather the difference in total enthalpy, which is dominated by the interlayer energy. Cruz et al. (1972) showed that the interlayer bonding is related primarily to the electrostatic energy contribution and only secondarily to hydrogen bond energy. Our study suggests that the interlayer bonding energy decreases in magnitude in the order kaolinite, dickite, and nacrite. This trend follows the hydrogen bond energy of Brindley et al. (1986) and Frost (1997) but is contrary to the trend of Prost et al. (1985).

The ambiguity between interlayer energy and interlayer cohesion can also be seen in the dehydroxylation phenomena (Fig. 5). Two parameters influence dehydroxylation, the geometry of the interlayer space (as a barrier to diffusion) and the bonding energy of the OH groups. The polytypes present different reaction mechanisms. Nacrite and dickite both decompose in two stages, a primary dehydroxylation around 800 K followed by a second one at 940 K. The dehydroxylation of the last OH at 940 K in dickite is in agreement with the infrared observation of Frost and Vassallo (1996) who mention the formation of an intermediate more stable silanol group. Nacrite appears to have a behavior intermediate between kaolinite and dickite. The temperature of the onset of dehydroxylation increases in the order halloysite, poorly ordered kaolinite, well-ordered kaolinite, nacrite, and dickite. The relatively open space of halloysite explains its early dehydroxylation. However, the dehydroxylation temperatures of nacrite and dickite do not match the interlayer energy trend but follow the cohesion trend coming from the intercalation of hydrazine study. There is a mismatch between structural stability and the thermodynamic stability.

It is proposed that the occurrence of the polymorphs is due to the competition between thermodynamic stability and interlayer cohesion. The interlayer cohesion is related to the properties of the layer surface. Further study of the surface and hydration properties of the polymorphs is needed to constrain their genesis.

ACKNOWLEDGMENTS

The authors thank M.D. Buatier, Université de Lille, and G.Y. Jeong, Andong National University, for kindly providing samples, E. Vicenzi for help with the microprobe analyses, D. Yates for help with the X-ray diffraction, and D.D. Moore for helpful suggestions. The paper was improved by the review from E. Smelik and editorial advice from J.W. Carey. This research was made possible by the Department of Energy (DOE grants DE-FG02-85ER 13747 and DE-FG03-97OR SF14749). The Thermochemistry Facility infrastructure is supported by the Center for High Pressure Research (CHiPR) an NSF Science and Technology Center and by the University of California at Davis.

REFERENCES CITED

Anovitz, L.M., Perkins, D., and Essene, E.J. (1991) Metastability in near-surface rocks of minerals in the system Al_2O_3-SiO_2-H_2O. Clays and Clay Minerals, 39, 225–233.

Artioli, G., Bellotto, M., Gualtieri, A., and Pavese, A. (1995) Nature of structural disorder in natural kaolinites: a new model based on computer simulation of powder diffraction data and electrostatic energy calculation. Clays and Clay Minerals, 43, 438–445.

Barany, R. and Kelley, K.K. (1961) Heats and free energies of formation of gibbsite, kaolinite, halloysite and dickite. U.S. Bureau of Mines Report of Investigation, 5825, 13 p.

Berman, R.G. (1988) Internally consistent thermodynamic data set for minerals in the system Na_2O-K_2O-CaO-MgO-FeO-Fe_2O_3-Al_2O_3-SiO_2-TiO_2-H_2O-CO_2. Journal of Petrology, 29, 445–522.

Bish, D.L. and von Dreele, R.B. (1989) Rietveld refinement of non-hydrogen atomic positions in kaolinite. Clays and Clay Minerals, 37, 289–296.

Bookin, A.S., Drits, V.A., Plancon, A., and Tchoubar, C. (1989) Stacking faults in kaolin-group minerals in the light of real structural features. Clays and Clay Minerals, 37, 297–307.

Brindley, G.W. (1980) Order and disorder in clay mineral structures. In G. Brown, Ed., The X-ray identification and crystal structures of clay minerals. Mineralogical Society, London.

Brindley, G.W. and Nakahira, M. (1959) X-ray diffraction and gravimetric study of the dehydration reactions of gibbsite. Zeitschrift für Kristallographie, 112, 136–149.

Brindley, G.W., Kao, C.C., Harrison, J., Lipsicas, M., and Raythatha, R. (1986) Relation between structural disorder and other characteristics of kaolinites and dickites. Clays and Clay Minerals, 34, 239–249.

Buatier, M.D., Potdevin, J.L., Lopez, M., and Petit, S. (1996) Occurrence of nacrite in the Lodève Permian basin (France). European Journal of Mineralogy, 8, 847–852.

Chai, L. and Navrotsky, A. (1993) Thermochemistry of carbonate-pyroxene equilibria. Contribution in Mineralogy and Petrology, 114, 139–147.

Circone, S. and Navrotsky, A. (1992) Substitution of $^{[6,4]}$Al in phlogopite: High-temperature solution calorimetry, heat capacities, and thermodynamic properties of the phlogopite-eastonite join. American Mineralogist, 77, 1191–1205.

Clemens, J.D., Circone, S., Navrotsky, A., McMillan, P.F., Smith, B.K., and Wall, V.J. (1987) Phlogopite: High temperature solution calorimetry, thermodynamic properties, Al-Si and stacking disorder, and phase equilibria. Geochimica and Cosmochimica Acta, 51, 2569–2578.

Cruz, M.I., Jacobs, H., and Fripiat, J.J. (1972) The nature of interlayer bonding in kaolin minerals. Proceedings of the International Clay Conference, Madrid, 35–44.

Cruz-Complido, M., Sow, C., and Fripiat, J.J. (1982) Spectre infrarouge des hydroxyles, cristallinité et énergie de cohésion des kaolins. Bulletin Minéralogique, 105, 493–498.

Devidal, J.L., Dandurand, J.L., and Gout, R. (1996) Gibbs free energy of formation of kaolinite from solubility measurement in basic solution between 60 and 170°C. Geochimica et Cosmochimica Acta, 60, 553–564.

Ehrenberg, S.N., Aagaard, P., Wilson, M.J., Fraser, A.R., and Duthie, D.M.L. (1993) Depth-dependent transformation of kaolinite to dickite in sandstones of the norwegian continental shelf. Clay Minerals, 28, 325–352.

Fripiat, J., Cases, J., Francois, M., and Letellier, M. (1982) Thermodynamic and microdynamic behavior of water in clay suspensions and gels. Journal of Colloid and Interface Science, 89, 378–400.

Frost, R.L. (1997) The structure of the kaolinite minerals: a FT-Raman study. Clay Minerals, 32, 65–77.

Frost, R.L. and Vassallo, M. (1996) The dehydroxylation of the kaolinite clay minerals using infrared emission spectroscopy. Clays and Clay Minerals, 44, 635–651.

Giese, R.F. (1988) Kaolin minerals: Structures and stabilities. In Mineralogical Society of America Reviews in Mineralogy, 19, 29–66.

Hemingway, B.S. and Robie, R.A. (1977) Enthalpies of formation of low albite, NaAlSi3O8, gibbsite, (Al(OH)3), and NaAlO2; revised values for $\Delta H^0_{f,298}$ and $\Delta G^0_{f,298}$ of some aluminosilicate minerals. U.S. Geological Survey Journal of Research, 5, 797–806.

Hemingway, B.S., Robie, R.A., and Kittrick, J.A. (1978) Revised values for the Gibbs free energy of formation of [$Al(OH_4)$-aq], diaspore, boehmite and bayerite at 298.15 K and 1 bar, the thermodynamic properties of kaolinite to 800 K and 1 bar, and the heats of solution of several gibbsite samples: Geochimica Cosmochimica Acta, 42, 1533–1543.

Iwata, S., Izumi, F., and Tsukamoto, A. (1989) Differential heat of water adsorption for montmorillonite, kaolinite and allophane. Clay Minerals, 24, 505–512.

Jeong, G.Y. and Kim, S.J. (1993) Boxwork fabric of halloysite-rich kaolin formed by weathering of anorthosite in the Sancheong area, Korea. Clays and Clay Minerals, 41, 56–65.

———(1996) Morphology of halloysite particles and aggregates in the weathering of anorthosite. Journal of the Mineralogical Society of Korea, 9, 64–70.

King, E.G. and Weller, W.W. (1961) Low-temperature heat capacities and entropies at 298.15°K of diaspore, kaolinite, dickite and halloysite: U.S. Bureau of Mines Report of Investigation, 5810, 6 p.

Kiseleva, I., Navrotsky, A., Belitsky, I.A., and Fursenko, B.A. (1996a) Thermochemistry and phase equilibria in calcium zeolites. American Mineralogist, 81, 658–667.

———(1996b) Thermochemistry of natural potassium sodium calcium leonhardite and its cation-exchanged forms. American Mineralogist, 81, 668–675.

Kittrick, J.A. (1966) Free energy of formation of kaolinite from solubility measurements. American Mineralogist, 51, 1457–1466.

———(1970) Precipitation of kaolinite at 25°C and 1 atm. Clays and Clay Minerals, 18, 261–267.

McHale, J.M., Navrotsky, A., and Perrotta, A.J. (1997) Effects of increased surface area and chemisorbed H_2O on the relative stability of nanocrystalline γ-Al_2O_3 and α-Al_2O_3. Journal of Physical Chemistry B, 101, 603–613.

Murray, H.H. (1988) Kaolins minerals: their genesis and occurrences. In Mineralogical Society of America Reviews in Mineralogy, 19, 67–90.

Navrotsky, A. (1997) Progress and new directions in high temperature calorimetry revisited. Physics and Chemistry of Minerals, 24, 222–241.

Navrotsky, A., Rapp, R., Smelik, E., Burnley, P., Circone, S., Chai, L., Bose, K., and Westrich, H. (1994) The behavior of H_2O and CO_2 in high-temperature lead borate solution calorimetry of volatile-bearing phases. American Mineralogist, 79, 1099–1109.

Prost, R. (1984) Etude par spectroscopie infrarouge à basse température des groupes OH de structure de la kaolinite, de la dickite et de la nacrite. Agronomie, 4, 403–406.

Prost, R., Damême, A., Huard, E., and Driard, J. (1985) Infrared study of structural OH in kaolinite, dickite, and nacrite at 300 to 5 K. In L.G. Shultz, H. Van Olphen, and F.A. Mumpton, Eds., Proceeding of the International Clay Conference, Denver, 456 p. The Clay Minerals Society, Bloomington, Indiana.

Reed, B.L. and Hemley, J.J. (1966) Occurrence of pyrophyllite in the Kekiktuk conglomerate, Brooks Range, northeastern Alaska. U.S. Geological Survey Professional Paper, 550-C, 162–166.

Robie, R.A. and Hemingway, B.S. (1991) Heat capacities of kaolinite from 7 to 380 K and of DMSO-intercalated kaolinite from 20 to 310 K. The entropy of kaolinite $Al_2Si_2O_5(OH)_4$. Clays and Clay Minerals, 39, 362–368.

———(1995) Thermodynamic properties of minerals and related substances at 298.15 K and 1 bar (10^5 pascals) and at higher temperatures. U.S. Geological Survey Bulletin, 2131, 461 p.

Robinson, G.R., Haas, J.L. Jr., Schafer, C.M., and Haselton, H.T. (1982) Thermodynamic and thermophysical properties of selected phases in the MgO-SiO_2-H_2O-CO_2, CaO-Al_2O_3-SiO_2-H_2O-CO_2, and Fe-Fe_2O_3-SiO_2 chemical systems, with special emphasis on the properties of basalts and their mineral components. U.S. Geological Survey Open-File Report, 83–79, 429 p.

Schroeder, P.A. and Pruett, R.J. (1996) Fe ordering in kaolinite: insights from ^{29}Si and ^{27}Al MAS NMR spectroscopy. American Mineralogist, 81, 26–38.

Singh, B. (1996) Why does halloysite roll? A new model. Clays and Clay Minerals, 44, 191–196.

Singh, B. and Mackinnon, I.D.R. (1996) Experimental transformation of kaolinite to halloysite. Clays and Clay Minerals, 44, 825–834.

Smelik, E.A., Jenkins, D.M., and Navrotsky, A. (1994) A calorimetric study of synthetic amphiboles along the tremolite-tschermakite join and the heats of formation of magnesiohornblend and tschermakite. American Mineralogist, 79, 1110–1122.

Van Olphen, H. and Fripiat, J.J.. (1979) Data Handbook for Clays and Other Non-Metallic Materials, 346 p. Pergamon Press, Oxford, U.K.

Zheng, H. and Bailey, W. (1994) Refinement of nacrite structure. Clays and Clay Minerals, 42, 46–52.

Zotov, A., Mukhamet-Galeev, A., and Schott, J. (1998) An experimental study of kaolinite and dickite relative stability at 150–300 °C and the thermodynamic properties of dickite. American Mineralogist, 83, 516–524.

Manuscript received January 23, 1998
Manuscript accepted October 5, 1998
Paper handled by J. William Carey

APPENDIX TABLE 1. Thermodynamic cycles used to calculate the enthalpy of drop solution of some impurities: (all values in kJ/mol)

Water	
2/3 Gibbsite (xl, 298 K) = 1/3 Al_2O_3 (sol, 975 K) + H_2O (gas, 975 K)	(1)[a]
1/3 Al_2O_3 (sol, 975 K) = 1/3 Al_2O_3 (xl, 298 K)	(2)[a]
H_2O (l, 298 K) + 1/3 Al_2O_3 (xl, 298 K) = 2/3 Gibbsite (xl, 298 K)	(3)[b]
H_2O (l, 298 K) = H_2O (gas, 975 K)	(4)
$\Delta H_4 = \Delta H_1 + \Delta H_2 + \Delta H_3$	
$= 2/3*184.5 - 1/3*107.2 - 2/3*26.55 = 69.6\ (\pm 1.1)$	
Anatase	
Rutile (xl, 298 K) = TiO_2 (sol, 975 K)	(5)[c]
Rutile (xl, 298 K) = Anatase (xl, 298 K)	(6)[b]
Anatase (xl, 298 K) = TiO_2 (sol, 975 K)	(7)
$\Delta H_7 = \Delta H_5 - \Delta H_6 = 55.4\ (\pm 1.2) - 5.3\ (\pm 2.2) = 50.1\ (\pm 2.5)$	
Alunite	
$KAl_3(OH)_6(SO_4)_2$ (xl, 298 K) = 1/2 K_2O (xl, 298 K) + 3/2 Al_2O_3 (xl, 298 K) + 3 H_2O(lq, 298 K) + 2 SO_2 (gas, 298 K) + O_2 (gas, 298 K)	(8)[b]
3 H_2O (lq, 298 K) = 3 H_2O (gas, 975 K)	(9)[b]
1/2 K_2O (xl, 298 K) = 1/2 K_2O (sol, 975 K)	(10)[d]
3/2 Al_2O_3 (xl, 298 K) = 3/2 Al_2O_3 (sol, 975 K)	(11)[a]
2 SO_2 (gas, 298 K) = 2 SO_2 (gas, 975 K)	(12)[b]
O_2(gas, 298 K) = O_2(gas, 975 K)	(13)[b]
$KAl_3(OH)_6(SO_4)_2$ (xl, 298 K) = 1/2 K_2O (sol, 975 K) + 3/2 Al_2O_3 (sol, 975 K) + 3 H_2O (gas, 975 K) + 2 SO_2 (gas, 975 K) + O_2(gas, 975 K)	(14)
$\Delta H_{14} = \Delta H_8 + \Delta H_9 + \Delta H_{10} + \Delta H_{11} + \Delta H_{12} + \Delta H_{13}$	
$= 1032 \pm 3*69.0 - 1/2*193.7 + 3/2*107.2 + 2*33.0 + 21.8$	
$= 1391\ (\pm 5)$	

Note: a = this work; b = Robie and Hemingway (1995); c = R.L. Putnam (personal communication); d = Kiseleva et al. (1996b).